Alternative representations of the correlation energy in density-functional theory: A kinetic-energy based adiabatic connection

Andrew M. Teale,[*,†,‡] Trygve Helgaker,[‡] and Andreas Savin[¶,§]

†*School of Chemistry, University of Nottingham, University Park, Nottingham NG7 2RD, United Kingdom*

‡

Centre for Theoretical and Computational Chemistry, Department of Chemistry, University of Oslo, P.O. Box 1033 Blindern, N-0315 Oslo, Norway

¶

Sorbonne Universités, UPMC Univ Paris 06, UMR 7616, Laboratoire de Chimie Théorique, F-75005 Paris, France

§*CNRS, UMR 7616, Laboratoire de Chimie Théorique, F-75005 Paris, France*

E-mail: andrew.teale@nottingham.ac.uk

Abstract

The adiabatic-connection framework has been widely used to explore the properties of the correlation energy in density-functional theory. The integrand in this formula may be expressed in terms of the electron–electron interactions directly, involving intrinsically two-particle expectation values. Alternatively, it may be expressed in terms of the kinetic energy, involving only one-particle quantities. In this work, we explore this alternative representation for the correlation energy and highlight some of its potential for the construction of new density functional approximations. The kinetic-energy based integrand is effective in concentrating static correlation effects to the low interaction strength regime and approaches zero asymptotically, offering interesting new possibilities for modelling the correlation energy in density-functional theory.

Introduction

The Kohn–Sham variant of density-functional theory (DFT)[1,2] is now the most widely applied methodology for electronic-structure calculations. In the 50 years since its conception, the range of molecular and solid-state properties to which is may be applied has grown enormously (see Refs.[3,4] for some recent perspectives). In all of these applications, the choice of approximate exchange–correlation functional is a governing factor in the accuracy that may be obtained from the simulations. Unfortunately, Kohn–Sham exchange–correlation functionals do not have the hierarchical systematicity of conventional *ab initio* approaches.[5] The development of new functionals therefore remains an active area of research and new perspectives / insights into the nature of the exact functional are of great value.

A particularly useful tool for understanding Kohn–Sham exchange–correlation functionals has been the adiabatic-connection (AC) formalism.[6–8] This formalism underpins the development of hybrid functionals and (in a modified form[9]) range-separated hybrids,[10,11] some of the most successful types of functional in use today. As well as providing a formal justification for these functionals, the AC can be used as a tool to study the behaviour of the exact functional—see, for example, Refs.[12–14] From this perspective, alternative models for the challenging exchange–correlation energy have been proposed[15–18] and tested against accurate *ab initio* models. The utility of the AC formalism in this context stems from the fact that it provides a direct and simple bridge between the Kohn–Sham model system of non-interacting particles (described by a single Slater determinant) and the complex physical interacting system (described by the full configuration-interaction wave function), at constant electronic density. It therefore provides a key link between Kohn–Sham models and accurate, systematically refineable, *ab initio* methods. For an extensive review of the AC formalism, see Ref.[19]

In the present article, we focus on the correlation component of the energy via the AC formalism. The exchange component can be readily expressed directly in terms of Kohn–Sham orbitals and so we do not consider it further. Instead, we consider two possible AC

representations of the correlation energy, comparing and contrasting their properties and the different opportunities they afford for the construction of practical computational models.

Adiabatic Connection Integrands

In the traditional approach to the electronic correlation problem in Kohn–Sham DFT,[2] the correlation energy is expressed through the AC formalism[6–8] in terms of expectation values of a series of partially interacting wave functions over two-particle operators. Specifically, the Hamiltonian

$$H_\lambda = T + V_\lambda + \lambda W \tag{1}$$

is introduced where λ is the interaction strength, T is the operator for the kinetic energy, W is the electron–electron interaction operator, and V_λ is an effective external potential that keeps the electron density constant for all values of λ between 0 (the Kohn–Sham system) and 1 (the physical system). In terms of the ground-state wave function Ψ_λ of H_λ, the correlation energy for the fictitious system defined by H_λ is given by

$$E_{\mathrm{c},\lambda} = \langle\Psi_\lambda|H_\lambda|\Psi_\lambda\rangle - \langle\Psi_0|H_\lambda|\Psi_0\rangle. \tag{2}$$

Using the Hellmann–Feynman theorem and the invariance of the density with λ, we obtain (assuming no degeneracy)

$$E_\mathrm{c} = E_{\mathrm{c},\lambda=1} = \int_0^1 (\langle\Psi_\lambda|W|\Psi_\lambda\rangle - \langle\Psi_0|W|\Psi_0\rangle)\ \mathrm{d}\lambda, \tag{3}$$

where the dependence of the integrand $\langle\Psi_\lambda|W|\Psi_\lambda\rangle - \langle\Psi_0|W|\Psi_0\rangle$ on λ is a guide in the development of density-functional approximations.

Whilst conceptually straightforward, the evaluation of the expectation values $\langle\Psi_\lambda|W|\Psi_\lambda\rangle$ requires the reduced second-order density matrices associated with the wave functions Ψ_λ. Most practical implementations of DFT employ the Kohn–Sham scheme, using the $\lambda = 0$

system of non-interacting fermions as a reference. In this case, the Hamiltonian $H_{\lambda=0}$ contains only single-particle operators, although the effective potential V_λ does reflect correlation effects, being determined to keep the Kohn–Sham electronic density fixed at that of the physical ($\lambda = 1$) system.

An Alternative Representation of the Correlation Energy

We now consider an alternative AC perspective for analysis of the electronic correlation energy in DFT, which only requires expectation values of one-particle operators. Whilst this perspective may seem awkward at first glance, it should be noted that the one-particle density matrix does encode correlation effects, as illustrated by, for example, the virial theorem. Given that we make explicit use only of one-particle operators in Kohn–Sham theory, such an alternative perspective may be useful for constructing density-functional approximations (or reduced first-order density-matrix approximations), avoiding all quantities involving the reduced second-order density matrix.

An expression for the correlation energy in Kohn–Sham theory in terms of a one-electron operator can be derived as follows.[20–23] Differentiating $E_{\mathrm{c},\lambda}$ in Eq. (2) and the corresponding expression for $E_{\mathrm{c},\lambda}/\lambda$ with respect to λ, we obtain, respectively, the two expressions

$$E'_{\mathrm{c},\lambda} = \langle \Psi_\lambda \, | W + V'_\lambda | \, \Psi_\lambda \rangle - \langle \Psi_0 \, | W + V'_\lambda | \, \Psi_0 \rangle \,, \tag{4}$$

$$\left(\frac{E_{\mathrm{c},\lambda}}{\lambda} \right)' = \left\langle \Psi_\lambda \left| -\frac{T}{\lambda^2} + \left(\frac{V_\lambda}{\lambda} \right)' \right| \Psi_\lambda \right\rangle - \left\langle \Psi_0 \left| -\frac{T}{\lambda^2} + \left(\frac{V_\lambda}{\lambda} \right)' \right| \Psi_0 \right\rangle . \tag{5}$$

Noting that the terms involving V_λ depend only on the density and are therefore independent of λ, we obtain the simplified expressions

$$E'_{\mathrm{c},\lambda} = \langle \Psi_\lambda \, | W | \, \Psi_\lambda \rangle - \langle \Psi_0 \, | W | \, \Psi_0 \rangle \,, \tag{6}$$

$$\left(\frac{E_{\mathrm{c},\lambda}}{\lambda} \right)' = -\frac{\langle \Psi_\lambda \, | T | \, \Psi_\lambda \rangle - \langle \Psi_0 \, | T | \, \Psi_0 \rangle}{\lambda^2} \,. \tag{7}$$

Integrating both sides of these equations with respect to λ from 0 to 1, we find that the left-hand side in both cases becomes the Kohn–Sham correlation energy E_c:

$$\int_0^1 E'_{\mathrm{c},\lambda}\,\mathrm{d}\lambda = E_{\mathrm{c},1} - E_{\mathrm{c},0} = E_\mathrm{c}, \tag{8}$$

$$\int_0^1 \left(\frac{E_{\mathrm{c},\lambda}}{\lambda}\right)'\mathrm{d}\lambda = E_{\mathrm{c},1} - \lim_{\lambda\to 0}\frac{E_{\mathrm{c},\lambda}}{\lambda} = E_\mathrm{c} - \lim_{\lambda\to 0}\frac{E'_{\mathrm{c},\lambda}}{\lambda'} = E_\mathrm{c}, \tag{9}$$

where in Eq. (8) we have used $E_{\mathrm{c},0} = 0$ according to Eq. (6), whereas in Eq. (9) we have used L'Hôpital's rule and then $E'_{\mathrm{c},0} = 0$ according to Eq. (7). Introducing the notation

$$W_{\mathrm{c},\lambda} = \langle\Psi_\lambda\,|W|\,\Psi_\lambda\rangle - \langle\Psi_0\,|W|\,\Psi_0\rangle\,, \tag{10}$$

$$T_{\mathrm{c},\lambda} = \langle\Psi_\lambda\,|T|\,\Psi_\lambda\rangle - \langle\Psi_0\,|T|\,\Psi_0\rangle\,, \tag{11}$$

$$\overline{T}_{\mathrm{c},\lambda} = -\lambda^{-2}T_{\mathrm{c},\lambda}, \tag{12}$$

we arrive at the following alternative AC representations of the correlation energy:

$$E_\mathrm{c} = \int_0^1 W_{\mathrm{c},\lambda}\,\mathrm{d}\lambda = \int_0^1 \overline{T}_{\mathrm{c},\lambda}\,\mathrm{d}\lambda. \tag{13}$$

In the following, we examine and compare the AC integrands $W_{\mathrm{c},\lambda}$ and $\overline{T}_{\mathrm{c},\lambda}$ for a few atomic and molecular systems.

Models of the Correlation Energy

For the conventional AC representation of the correlation energy, it has been profitable to consider how the integrand $W_{\mathrm{c},\lambda}$ may be modelled. Such models lead directly to forms for the correlation energy via integration, providing a framework for developing new correlation functionals. In this work, we consider the following simple formula for the correlation energy

at interaction strength λ, guided by second-order perturbation theory[18]:

$$\varepsilon_{\mathrm{D},\lambda} = -\frac{w^2\lambda^2}{h + g\lambda}. \tag{14}$$

Here the parameter w represents the interaction of the noninteracting Kohn–Sham state with excited states, the parameter $h > 0$ models the HOMO–LUMO gap in the noninteracting limit, whereas the parameter $g > 0$ models the opening of the HOMO–LUMO gap for interacting systems.[18] Introducing the assumption that $w = g$, differentiation with respect to λ of $\varepsilon_{\mathrm{D}}(\lambda)$ and $\varepsilon_{\mathrm{D}}(\lambda)/\lambda$ then yields the following formulas for the AC integrands:

$$W_{\mathrm{D},\lambda} = -\frac{g^2\lambda(2h + g\lambda)}{(h + g\lambda)^2}, \quad W'_{\mathrm{D},\lambda} = -\frac{2g^2h^2}{(h + g\lambda)^3}, \tag{15}$$

$$\overline{T}_{\mathrm{D},\lambda} = -\frac{g^2h}{(h + g\lambda)^2}, \qquad \overline{T}'_{\mathrm{D},\lambda} = \frac{2g^3h}{(h + g\lambda)^3}. \tag{16}$$

The AC model integrands have the following noninteracting and strictly interacting limits:

$$W_{\mathrm{D},0} = 0, \qquad W_{\mathrm{D},\infty} = -g, \tag{17}$$

$$\overline{T}_{\mathrm{D},0} = -\frac{g^2}{h}, \quad \overline{T}_{\mathrm{D},\infty} = 0. \tag{18}$$

We also note the following revealing relationship between their first derivatives

$$\overline{T}'_{\mathrm{D},\lambda} = -\frac{g}{h}W'_{\mathrm{D},\lambda}. \tag{19}$$

The model AC integrands $W_{\mathrm{D},\lambda}$ and $\overline{T}_{\mathrm{D},\lambda} = -\lambda^2 T_{\mathrm{D},\lambda}$ are therefore monotonically decreasing and increasing functions of λ, respectively, towards the strictly-correlated limit, which in the case of $\overline{T}_{\mathrm{D},\lambda}$ is zero.

Computational Details

In this paper, we present AC curves of the two integrands in Eq. (13), obtained from accurate *ab initio* calculations. Accurate values for the integrands are determined using the approach of Refs.[13,14] with coupled-cluster wave functions at the coupled-cluster singles-and-doubles (CCSD) level for the two-electron systems and coupled-cluster singles-doubles-perturbative-triples [CCSD(T)] level for the four-electron systems studied. We note that the CCSD model is equivalent to the full configuration-interaction (FCI) model for the two-electron systems. For comparison, the integrands corresponding to the Perdew–Burke–Ernzerhof (PBE)[24] density-functional approximation have also been determined, using scaling relations.[25] The PBE integrands are evaluated for the same (FCI or CCSD(T)) densities as the accurate *ab initio* integrands.

All calculations have been carried out using the uncontracted aug-cc-pVTZ basis set[26,27] for both the orbital and potential expansions. A development version of the DALTON quantum-chemistry program[28,29] has been used for all calculations in this work. All electrons are correlated in the coupled-cluster calculations and the electronic densities are determined via the Lagrangian approach of Helgaker and Jørgensen, including orbital relaxation terms.[30,31] The results obtained for the atomic systems are consistent with the earlier study of Colonna and Savin.[12] To aid with reproducibility of the AC curves, we have fitted analytic functions based on the second-order perturbation-theory inspired model of Teale, Coriani, and Helgaker[18] to the calculated data. The values of the fitted parameters g and h in Eq. (14) are given in the Appendix.

We have studied the helium isoelectronic series with nuclear charge $2 \leq Z \leq 10$, the beryllium isoelectronic series with $4 \leq Z \leq 10$, and the H_2 molecule at the internuclear separations 0.7, 1.4, 3.0, 5.0, 7.0, and 10.0 bohr. These prototypical systems allow us to explore a range of correlation effects. Dynamic correlation is captured by the helium isoelectronic series, near-degeneracy effects by the beryllium isoelectronic series, and the transition from dynamic to static correlation by the H_2 molecule at different internuclear separation.

Results

AC Integrands for Helium and Beryllium Isoelectronic Series

We begin by considering the conventional AC integrand $W_{c,\lambda}$, which features the electron–electron interactions explicitly. Figure 1 shows that, in certain cases, $W_{c,\lambda}$ is well reproduced by simple approximations such as the PBE functional.[24] In the left-hand panel of Figure 1, $W_{c,\lambda}$ is shown for helium isoelectronic atoms with $Z = 2, 6, 10$, whereas $W_{c,\lambda}$ for the beryllium isoelectronic series with $Z = 4, 7, 10$ is shown in the right-hand panel. The *ab initio* integrands are plotted with solid lines, whilst the corresponding PBE curves are dashed. For both series, the PBE functional provides a reasonable approximation at low Z values but deteriorates as Z increases.

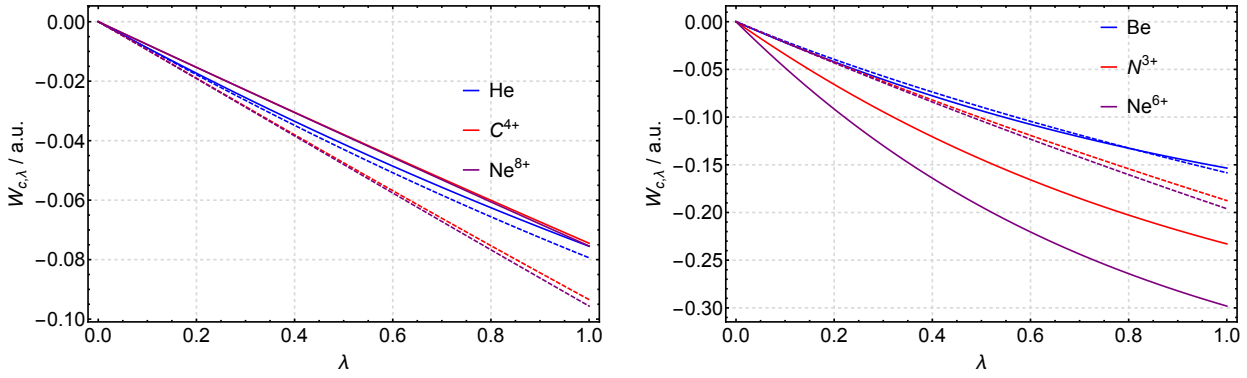

Figure 1: The AC integrand $W_{c,\lambda}$ for the helium isoelectronic series (left panel) and beryllium isoelectronic series (right panel). Accurate *ab initio* integrands are shown as full lines, those corresponding to the PBE approximation are shown by dashed lines.

In the helium isoelectronic series, the PBE approximation captures the tendency of the $W_{c,\lambda}$ integrand towards linearity as Z increases. However, the *ab initio* and PBE integrands behave differently with increasing Z. Whereas the *ab initio* curves give a less negative correlation energy with increasing Z in the helium series, the PBE curves give a more negative correlation energy with increasing Z. It should be noted that in Ref.[14] the trend for the *ab initio* curves is reversed in larger basis sets. The present trend may therefore reflect a limitation of the basis set used in this work. Nonetheless, it is clear that the

PBE integrands and associated correlation energies tend towards too negative values with increasing Z, noting that the PBE correlation energy for Ne^{8+} in this basis set is already 5 mE_h below the estimated basis-set limit value of Ref.[14]

For the beryllium isoelectronic series, a more pronounced failure is observed for the PBE approximation as Z increases—see, for example, Ne^{6+} in the right-hand panel of Figure 1. This failure has been connected to the near-degeneracy present in the beryllium isoelectronic series.[32] In the *ab initio* curves, the onset of the near-degeneracy is manifested by a more pronounced curvature of the integrand. This feature is not well reproduced by typical density-functional approximations.

Figure 2 shows the same systems as in Figure 1 but with the kinetic-energy AC integrand $\overline{T}_{c,\lambda} = -\lambda^{-2} T_{c,\lambda}$, see Eq. (13). For the helium series, the *ab initio* integrands are almost linear, with a very slight concave character. The PBE integrands show a qualitatively different character, being convex with a pronounced upturn at low λ, although, for $\lambda > 0.2$, the PBE curves become more parallel with the *ab initio* curves. For the beryllium series, the concavity of the *ab initio* curves becomes more pronounced with increasing Z. The PBE curves fail to reproduce this trend and show a similar (but less pronounced) upturn at low λ as in the helium series.

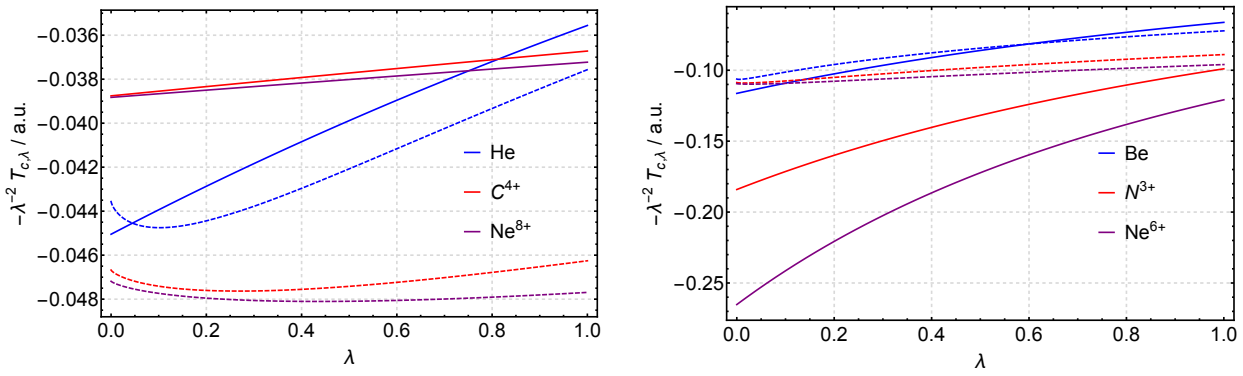

Figure 2: The AC integrand $-\lambda^{-2} T_{c,\lambda}$ for the helium isoelectronic series (left panel) and beryllium isoelectronic series (right panel). Accurate *ab initio* integrands are shown as full lines, those corresponding to the PBE approximation are shown by dashed lines.

The largest differences between the PBE and *ab initio* curves occur for N^{3+} and Ne^{6+}.

Interestingly, the errors in the PBE integrand increase with λ for $W_{c,\lambda}$, whereas the $\overline{T}_{c,\lambda}$ errors decrease with increasing λ. This behaviour leads to different prospects when approximating the two integrands. In particular, for the $\overline{T}_{c,\lambda}$ integrand, it may be profitable to consider partially interacting reference systems with $\lambda > 0$ as a starting point.

In this work, the AC integrands presented are derived by fitting Eqs. (15) and (16) to *ab initio* data. The fitted curves reproduce the DFT correlation energies to better than 10^{-6} E_h accuracy for all the systems considered; the corresponding coefficients are presented in the appendix. From Figures 1 and 2, the monotonically decreasing and increasing nature of the integrands $W_{D,\lambda}$ and $\overline{T}_{D,\lambda}$ is clear. An interesting point is that the $W_{D,\lambda}$ model integrand is convex. For the exact integrand, convexity in λ has not been proven, only monotonicity, although we have never observed a counter example based on accurate *ab initio* calculations. The model $\overline{T}_{D,\lambda}$ is similarly concave. However, close examination of the accurate *ab initio* data in the low-λ limit reveals that the kinetic-energy AC integrand can be non-concave. Whilst this has little impact on the accuracy of the correlation energy obtained by integration or the overall shape of the curve, it does mean that the relationship of Eq. (19) is not closely obeyed for the accurate derivatives. Thus, whilst the accurate first derivative of the integrand at $\lambda = 0$ is recovered by the convex $W_{D,\lambda}$, this is not the case for the concave $\overline{T}_{D,\lambda}$. Similar behaviour is observed also for the configuration-interaction inspired model of Ref.,[18] which is also convex/concave.

AC Integrands for the H_2 Molecule

The effect of near-degeneracy is further illustrated by stretching H_2, see Figures 3 and 4. Initially, for small values of λ, a rapid change is observed in both AC integrands. In both cases, the AC curves can be linearly extrapolated to a point beyond which a constant is a better approximation. Whereas this constant is unknown for $E'_{c,\lambda} = W_{c,\lambda}$, it is zero for $(E_{c,\lambda}/\lambda)' = \overline{T}_{c,\lambda}$ it can be set to zero, illustrating the different possibilities for modelling these integrands when developing new approximations. In particular, the parameterisation

of the AC integrand in terms of the kinetic energy may be advantageous for extrapolation.[33] This alternative parameterisation may also provide an interesting new perspective for the construction of double-hybrid functionals based on the AC.[34,35]

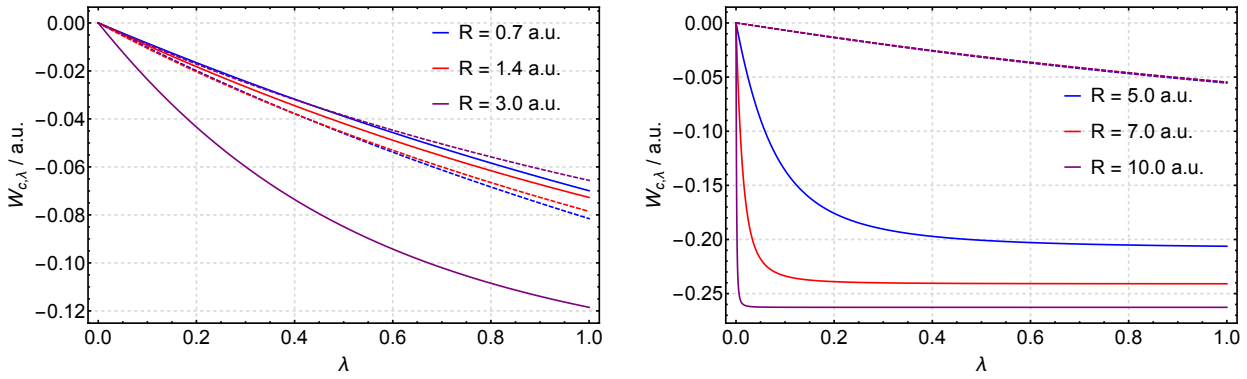

Figure 3: The AC integrand $W_{c,\lambda}$ for different internuclear distances in the H_2 molecule. E_c corresponds to the area of the shaded region. Accurate *ab initio* integrands are shown as full lines, those corresponding to the PBE approximation are shown by dashed lines.

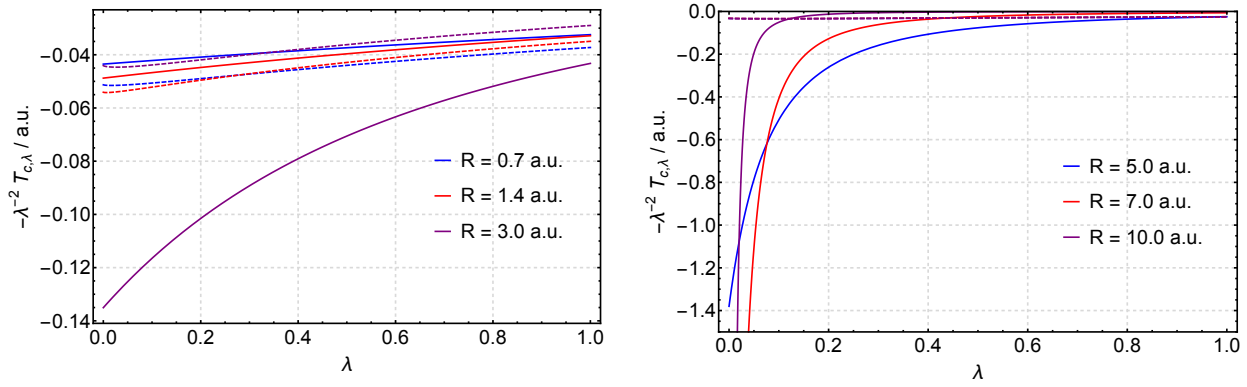

Figure 4: The AC integrand $-\lambda^{-2} T_{c,\lambda}$ for different internuclear distances in the H_2 molecule. E_c corresponds to the area of the shaded region. Accurate *ab initio* integrands are shown as full lines, those corresponding to the PBE approximation are shown by dashed lines.

In Figures 3 and 4, it is clear that the PBE approximation provides a reasonable description of both AC integrands in the dynamically correlated regime (internuclear separations $R = 0.7$ and 1.4 bohr) but becomes progressively worse as static correlation becomes more important with increasing internuclear separation. Qualitatively, the *ab initio* curves in Figure 4 resemble those for the beryllium series in Figure 2 as Z increases, indicating that near-degeneracy effects lead to a concentration of the integrand $\overline{T}_{c,\lambda}$ to low λ.

The non-concavity of $\overline{T}_{\mathrm{c},\lambda}$, as discussed in the previous section, is more pronounced as static correlation becomes important—for example, in H_2 at $R \geq 5.0$ a.u., suggesting that models including terms with higher-order λ contributions may be required. Such contributions may be incorporated by considering models inspired by higher-order perturbation theories, see Ref.[18] Such models remove the restriction to concave or convex behaviour. Further investigation of this aspect will be carried out in future work. In particular, a better description of this limit will be useful for the construction of Kohn–Sham correlation functionals based only on information available from the Kohn–Sham reference system. Alternatively, hybrid correlation approaches, which may be viewed as utilising a partially interacting reference with $\lambda > 0$, may be pursued as a route to circumvent modelling the more complex behaviour in the very low-λ regime.

Conclusions

Within the AC framework, the Kohn–Sham correlation energy can be computed in two alternative ways, either from the kinetic-energy integrand $\overline{T}_{\mathrm{c},\lambda} = -\lambda^{-2}\, T_{\mathrm{c},\lambda}$ or from the electron–electron integrand $W_{\mathrm{c},\lambda}$, see Eq. (13). Although the latter approach is much more commonly discussed, the first approach has the advantage of providing a framework where some features appear in a more natural way. By concentrating near-degeneracy effects into the region of small λ values, a perturbation treatment may be more appropriate and better suited to the development of models with partially interacting reference systems.

Perhaps the most striking and important advantage of the integrand $\overline{T}_{\mathrm{c},\lambda}$ is that its strong-interaction limit $\lambda \to \infty$ is simple, being equal to zero. This behaviour contrasts sharply with that of $W_{\mathrm{c},\lambda}$, where the corresponding limit requires a solution for strictly correlated electrons.[36] Even though significant progress has been made in understanding this limit in recent years,[37–40] the treatment of such systems is still difficult. The simple model of Eq. (16) and its relationship to the model of Eq. (15) suggests that the complexity

of the kinetic energy integrand may not be higher than that of the conventional integrand for other λ values. Combined with a trivial strong-interaction limit, this observation makes the kinetic-energy integrand an interesting quantity for further study and the development of practical numerical approximations.

Several avenues are possible for the development of practical computational schemes that make use of the alternative AC representation studied here. In analogy to Refs.[15–18] functionals can be constructed by considering interpolation schemes. In particular, if the interpolations are designed to obey the known limit $\overline{T}_{c,\infty} = 0$, then models can be constructed that depend only on quantities available in the Kohn–Sham limit ($\lambda = 0$), avoiding quantities calculated at finite interaction strengths. Just as in the standard AC representation, it may be necessary to consider local energy-density representations to maintain size-consistency of the approximate models, see Refs.[41,42] for detail discussion of this point. Work is presently underway in this direction for the standard AC representation and will be extended to this alternative representation. Recently, an alternative extrapolation approach has been put forward as a computational route to determine correlation energies[33] and has also been applied to the computation of excitation energies.[43] This alternative AC representation may also be useful when tailored to approach 0 for large λ, the tendency for static correlation to be concentrated towards low λ values meaning that extrapolations beginning from weakly interacting references, with small values of λ, may be accurate.

Finally, although not discussed in the present paper, we would like to point out that that the kinetic-energy operator only probes a region close to the diagonal of the reduced first-order density matrix, suggesting that local, or semi-local, approximations have a higher chance of success.

Appendix

In this work, we have presented conventional and kinetic-energy based AC integrands for

the correlation energy in Kohn–Sham DFT. Accurate *ab initio* methods have been used to calculate values of the integrands at a range of λ values between 0 and 1. For the conventional integrands, the form of the integrand in Eq. (15) was used, whilst for the kinetic-energy based integrand the form of Eq. (16) was employed. The parameters obtained by fitting these functions to *ab initio* data are presented in Table 1

Table 1: The fitted parameters g and h used in Eqs. (15) and (16) throughout this work.

Species	g	h
H_2 $R = 0.7$ a.u.	0.275443	1.743630
H_2 $R = 1.4$ a.u.	0.223365	1.022690
H_2 $R = 3.0$ a.u.	0.176083	0.229583
H_2 $R = 5.0$ a.u.	0.212446	0.032705
H_2 $R = 7.0$ a.u.	0.242801	0.006586
H_2 $R = 10.0$ a.u.	0.263190	0.000527
He	0.358771	2.857320
C^{4+}	1.527200	60.316000
Ne^{8+}	2.634780	180.143000
Be	0.357787	1.100440
N^{3+}	0.506110	1.391380
Ne^{6+}	0.550901	1.144380

Acknowledgement

A. M. T. is grateful for support from the Royal Society University Research Fellowship scheme. We are grateful for access to the University of Nottingham High Performance Computing Facility. This work was supported by the Norwegian Research Council through the CoE Centre for Theoretical and Computational Chemistry (CTCC) Grant No. 179568/V30 and through the European Research Council under the European Union Seventh Framework Program through the Advanced Grant ABACUS, ERC Grant Agreement No. 267683.

References

1. Hohenberg, P.; Kohn, W.; *Phys. Rev.* **1964**, *136*, 864B

2. Kohn, W.; Sham, L. J. *Phys. Rev.* **1965**, *140*, A1133

3. Burke, K.; *J. Chem. Phys.* **2012**, *136*, 150901

4. Becke, A. D.; *J. Chem. Phys.* **2014**, *140*, 18A301

5. Helgaker, T.; Jørgensen, P.; Olsen, J.; *Molecular Electronic-Structure Theory*, John Wiley & Sons Ltd., West Sussex, England, 2000

6. Harris, J.; Jones, R. O. *J. Phys. F* **1974**, *4*, 1170–1186

7. Langreth, D. C.; Perdew, J. P. *Solid State Commun.* **1975**, *17*, 1425

8. Gunnarsson, O.; Lundqvist, B. I. *Phys. Rev. B* **1976**, *13*, 4274

9. Yang, W.; *J. Chem. Phys.* **1998**, *109*, 10107

10. Savin, A.; *Beyond the Kohn-Sham determinant*, in Recent Advances in Density Functional Theory, edited by D. P. Chong, World Scientific, 1996.

11. Savin, A.; *On degeneracy, near degeneracy and density functional theory*, in Recent Developments of Modern Density Functional Theory, edited by J. M. Seminario, pages 327–357, Elsevier, Amsterdam, 1996.

12. Colonna, F.; Savin, A. *J. Chem. Phys.* **1999**, *110*, 2828

13. Wu, Q.; Yang, W. *J. Chem. Phys.* **2003**, *118*, 2498–2509

14. Teale, A. M.; Coriani, S.; Helgaker, T. *J. Chem. Phys.* **2009**, *130*, 104111

15. Seidl, M.; Perdew, J. P.; Kurth, S.; *Phys. Rev. Lett.* **2000**, *84*, 5070

16. Gori-GIorgi, P.; Vignale, G.; Seidl, M.; *J. Chem. Theory Comput.* **2009**, *5*, 743

17. Cohen, A. J.; Mori-Sanchéz, P.; Yang, W.; *J. Chem. Phys.* **2007**, *127*, 034101

18. Teale, A. M.; Coriani, S.; Helgaker, T. *J. Chem. Phys.* **2010**, *132*, 164115

19. Savin, A.; Colonna, F.; Pollet, R.; *Int. J. Quantum Chem.*, **2003**, *93*, 166

20. Yasuhara, H. *Lett. Nuovo Cimento* **1975**, *12*, 412

21. Savin, A. *Phys. Rev. A* **1995**, *52*, R1805

22. Levy, M.; Görling, A. *Phys. Rev. A* **1995**, *52*, 1808

23. Gersdorf, P.; John, W.; Perdew, J. P.; Ziesche, P. *Int. J. Quantum Chem.* **1997**, *61*, 935

24. Perdew, J. P.; Burke, K.; Ernzerhof, M. *Phys. Rev. Lett.* **1996**, *77*, 3865

25. Joubert, D. P.; Strivastava, G. P. *J. Chem. Phys.* **1998**, *109*, 5212

26. Dunning, T. H. *J. Chem. Phys.* **1989**, *90*, 1007

27. Kendall, R. A.; Dunning, T. H.; Harrison, R. J. *J. Chem. Phys.* **1992**, *96*, 6796

28. DALTON, a molecular electronic structure program, Release Dalton2015.0 (2015), see http://daltonprogram.org

29. K. Aidas and C. Angeli and K. L. Bak and V. Bakken and R. Bast and L. Boman and O. Christiansen and R. Cimiraglia and S. Coriani and P. Dahle and E. K. Dalskov and U. Ekström and T. Enevoldsen and J. J. Eriksen and P. Ettenhuber and B. Fernández and L. Ferrighi and H. Fliegl and L. Frediani and K. Hald and A. Halkier and C. Hättig and H. Heiberg and T. Helgaker and A. C. Hennum and H. Hettema and E. Hjerteniæs and S. Høst and I.-M. Høyvik and M. F. Iozzi and B. Jansík and H. J. Å. Jensen and D. Jonsson and P. Jørgensen and J. Kauczor and S. Kirpekar and T. Kjærgaard and W. Klopper and S. Knecht and R. Kobayashi and H. Koch and J. Kongsted and A. Krapp and K. Kristensen and A. Ligabue and O. B. Lutnæs and J. I. Melo and K. V. Mikkelsen and R. H. Myhre and C. Neiss and C. B. Nielsen and P. Norman and J. Olsen and J. M. H. Olsen and A. Osted and M. J. Packer and F. Pawlowski and T. B. Pedersen and P. F. Provasi and S. Reine and Z. Rinkevicius and T. A. Ruden and K. Ruud and V.

Rybkin and P. Sałek and C. C. M. Samson and A. Sánchez de Merás and T. Saue and S. P. A. Sauer and B. Schimmelpfennig and K. Sneskov and A. H. Steindal and K. O. Sylvester-Hvid and P. R. Taylor and A. M. Teale and E. I. Tellgren and D. P. Tew and A. J. Thorvaldsen and L. Thøgersen and O. Vahtras and M. A. Watson and D. J. D. Wilson and M. Ziolkowski and H. Åagren, *WIRES Comput. Mol. Sci.*, **2014**, *4*, 269

30. Jørgensen, P.; Helgaker, T.; *J. Chem. Phys.*, **1988**, *89*, 1560

31. Hald, K.; Halkier, A.; Jørgensen, P.; Coriani, S.; Hättig, C.; Helgaker, T.; *J. Chem. Phys.*, **2003**, *118*, 2985

32. Perdew, J. P.; McMullen, E. R.; Zunger, A. *Phys. Rev. A* **1981**, *23*, 2785

33. Savin, A. *J. Chem. Phys.* **2011**, *134*, 214108

34. Sharkas, K.; Toulouse, J.; Savin, A. *J. Chem. Phys.* **2011**, *134*, 064113

35. Cornaton, Y.; Franck, O.; Teale, A. M.; Fromager, E. *Mol. Phys.* **2013**, *111*, 1275

36. Seidl, M. *Phys. Rev. A* **1999**, *60*, 4387

37. Seidl, M.; Perdew, J. P.; Levy, M. *Phys. Rev. A* **1999**, *59*, 51

38. Seidl, M.; Gori-Giorgi, P.; Savin, A. *Phys. Rev. A* **2007**, *75*, 042511

39. Gori-Giorgi, P.; Vignale, G.; Seidl, M. *J. Chem. Theory Comput.* **2009**, *5*, 743

40. Mirtschink, A.; Seidl, M.; Gori-Giorgi, P. *J. Chem. Theory Comput.* **2012**, *8*, 3097

41. Gori-Giorgi, P.; Savin, A.; *J. Phys.: Conference Series*, **2008**, *117*, 012017

42. Savin, A.; *Chem. Phys.*, **2009**, *356*, 91

43. Rebolini, E.; Toulouse, J.; Teale, A. M.; Helgaker, T.; Savin, A.; *Phys. Rev. A*, **2015**, *91*, 032519

Table of Content (ToC) Graphical Abstract

Accurate adiabatic-connection curves with kinetic-energy integrand

Andrew M. Teale, Trygve Helgaker and Andreas Savin

A novel representation for the exchange–correlation energy in Kohn–Sham theory is investigated using *ab initio* methods. This approach places emphasis on the kinetic energy and the one-particle reduced density matrix, providing a potentially fruitful perspective for the development of new approximations.